First non-intercepting emittance measurement by means of optical diffraction radiation

interference

First non-intercepting emittance measurement by means of optical diffraction radiation interference

A Cianchi[1], V Balandin[2], M Castellano[3], E Chiadroni[3], L Catani[4], N Golubeva[2], K Honkavaara[2], G Kube[2] and M Migliorati[5]

[1] INFN-Roma Tor Vergata & University of Rome 'Tor Vergata', Via della Ricerca Scientifica, 1-00133 Rome, Italy
[2] DESY, Notkestrasse 85, 22607 Hamburg, Germany
[3] INFN-LNF, Via E. Fermi, 40-00044 Frascati, Rome, Italy
[4] INFN-Roma 'Tor Vergata', Via della Ricerca Scientifica, 1-00133 Rome, Italy
[5] Dept. SBAI, Sapienza University of Rome, Via A. Scarpa 16, 00161 Roma, Italy
E-mail: alessandro.cianchi@roma2.infn.it

Abstract

Transverse electron beam size measurements are required in order to determine the transverse emittance. In the case of high brightness electron beams produced by high repetition rate linear accelerators, conventional invasive diagnostics cannot sustain the intense power dissipated in intercepting devices. The analysis of the angular distribution of diffraction radiation has been proven to be a competent candidate for non-intercepting measurements of electron beam parameters. In addition, optical diffraction radiation interference (ODRI) has been demonstrated to be superior to the single slit ODR due to its shielding capability against the synchrotron radiation background and the possibility of avoiding complementary diagnostics. This paper reports the first transverse emittance measurement ever performed with the ODRI technique. In addition, the intrinsic non-intercepting and non-disturbing feature of the ODRI method has been checked in our experimental conditions by wakefield calculations.

Keywords: diffraction radiation, high brightness beam, emittance measurement

1. Introduction

High brightness or high repetition rate electron beams, mainly destined to serve as advanced radiation sources, are currently produced at several accelerator facilities worldwide, and more are foreseen in the near future. The transverse emittance measurement is of paramount importance in order to achieve the required high beam quality. Emittance measurements are usually based on the quadrupole scan or multiple screens technique [1]. Conventional intercepting devices, such as screens, mainly using optical transition radiation (OTR), or wire scanners, are widely used to measure the beam size in order to determine the emittance value. However, in the case of high brightness beams having small transverse dimensions—typically below 100 μm—or high repetition rate in the order of MHz, the energy deposited in the intercepting devices makes their use unfeasible.

The laser wire [2, 3] provides an attractive option; however it faces tight mechanical and optical requirements. Our approach is to use the angular distribution of far-field ODR, produced by an electron bunch passing through a rectangular aperture in a screen. This technique was proposed several years ago [4] as a non-intercepting device for beam size measurements. When the radial extension of the electromagnetic field (in the order of $\gamma\lambda$, where γ is the Lorentz factor and λ the wavelength of observation) is larger than the aperture size, the field interacts with the screen resulting in the emission of ODR. The use of a rectangular slit instead of a circular hole [5] has several advantages: it simplifies the mathematical treatment and eases the mechanical machining of the slit. The physics of the diffraction radiation emission, as well as the effects of the used geometry on the angular distribution of the emitted radiation has been described in [6] and later extensively treated in several papers, e.g. [7, 8], and in a recent book [9]. The first measurement of the beam size using ODR has been performed at KEK [10], demonstrating the potential of this technique but also highlighting some unwanted problems. For example, the synchrotron radiation (SR), mainly produced by the magnetic elements upstream of the beam size measurement location, is scattered around the beam pipe, distorting the low intensity signal produced by ODR. Furthermore, in order to avoid a systematic error in beam size measurements [4], standard ODR-based techniques require complementary diagnostics to align the electron beam into the center of the slit. The ODRI technique has been developed in order to overcome both problems. Standard emittance measurements using OTR imaging or wire scanners are, nevertheless, more easily implemented as measurements based on ODR, and therefore preferable when beam parameters allow them.

A detailed description of the ODRI physics including the used formulas and approximations can be found in [11]. We recall here only some basic features. In the traditional DR-based diagnostics, the angular distribution of the diffraction radiation, which is emitted when a charged particle beam passes a slit aperture, is detected. For ODRI measurements, an additional slit aperture with different size is used (see figure 1). The distance between the screens is shorter than the radiation formation length. The ODR emitted in the forward direction at the first slit interferes with the backward radiation produced at the second slit. Different slit apertures are needed in order to avoid signal cancellation due to destructive interference between the emitted fields. The interference pattern contains valuable information regarding the beam parameters: transverse size, angular divergence and relative position inside the slits can be retrieved from it. When using a single slit setup, it is not possible to distinguish the beam size and the beam position inside the slit, and a complementary diagnostic is needed in order to separate these two contributions. We have demonstrated in [11] that this is not the case
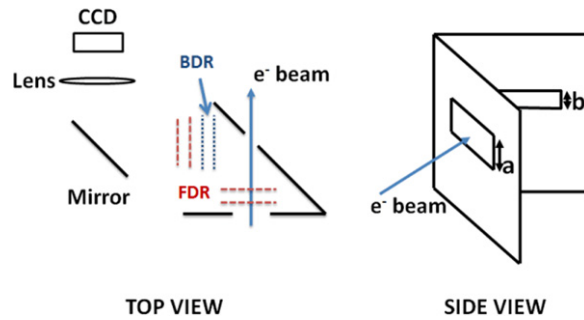
Figure 1. Sketch of the two-slit setup. Dimension a is the aperture size of the first slit; b is the size of the second slit. The FDR produced at the first interface is reflected and interferes with the BDR from the second surface. An optical system, described later in the paper, images the radiation onto a CCD device.

when using ODRI with non-collinear slits. This is an important difference because in our case we do not need any additional diagnostics to retrieve the beam position inside the slit, and also the contributions to the angular distribution of beam position and beam size are separated from each other. A more detailed analysis of the near fields in a real experimental geometry and the effects on the radiation angular distribution has recently been studied, demonstrating that our far field approximation is accurate if the misalignment of the slit centers is within $50\,\mu$m [12], consistent with our measurement setup. This result confirms the very good agreement between data and theoretical model shown in [11].

Another significant advantage of ODRI compared to ODR concerns the better efficiency in shielding against the SR background. The first screen acts as a mask, effectively reducing the SR background.

2. Experimental setup

A sketch of the used ODRI setup is shown in figure 1.

The first slit, 1 mm wide and normal to the beam direction, acts as a shield against the SR background. In addition, the forward ODR (FDR) produced by this slit interferes with the backward ODR (BDR) at the second interface, where an aperture of 0.5 mm is placed. The distance between the two screens is about 2 cm, much shorter than the formation length (in the order of $\gamma^2\lambda$) in the case of optical wavelengths and at 1 GeV electron beam energy. The difference in the aperture sizes prevents the complete cancellation of the fields, resulting in a clear interference pattern.

The experimental setup consists of an in-vacuum actuator used to insert an aluminum coated silicon screen into a precise position with respect to the electron beam axis. The screen holder is shown in figure 2. The 1 mm wide slit can also be moved using a dedicated second movable actuator allowing a remote control of the relative vertical position between the slits. The 0.5 mm slit aperture on the screen is opened by means of a lithographic technique using anisotropic etching in a KOH solution, allowing the creation of clean and very sharp edges. The manufacturing procedure has been described in [13]. With respect to our screen, the only difference from the one in [13] is the use of the silicon nitride as mask etching instead of silicon oxide, allowing a more uniform and slower etching rate.
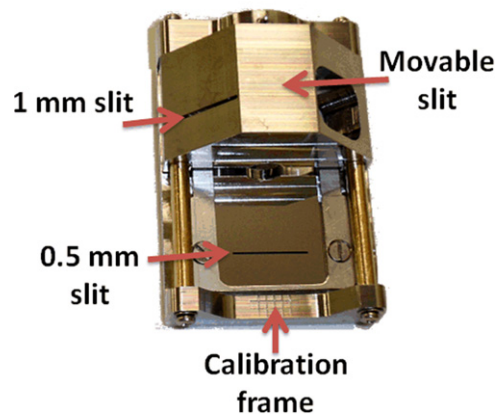
Figure 2. A picture of the screen holder. The movable 1 mm wide slit acts as SR shielding and an FDR target. The BDR generating screen has a 0.5 mm wide slit. A calibration pattern is visible on the bottom part of the frame. The central part can be used as a standard OTR screen.

Since the first slit can be moved vertically with respect to the second one, it is possible to measure ODRI angular distributions in the same experimental conditions with only one parameter, i.e. the offset of the electron beam with respect to the center of the first slit, changed in a controlled way. In addition, since the middle part of the second screen can be used as a conventional OTR screen, the ODRI results can be directly compared with those from OTR measurements.

The emitted radiation is extracted out of the beam pipe through a window, reflected by a mirror and guided into an optical system which can be moved remotely with respect to the optical axis. An achromatic doublet with focal length $f = 250$ mm is used to image the beam, while a custom apochromatic lens ($f = 531$ mm), designed to reduce the influence of the chromatic aberration, is implemented to obtain the ODRI angular distribution. Several narrow band interferential filters are mounted onto a filter wheel to select the observation wavelength. A second wheel is equipped with two Glan–Thomson polarizers to select vertical or horizontal polarization. The polarizer lengthens the optical path, thus increasing the focal length. This variation can be corrected by changing slightly the longitudinal camera position. The detector used is a cooled, high sensitivity, 16-bit CCD camera (Hamamatsu ORCA II-BT-512G model type C4742–98-26LAG2). The main advantages of this kind of camera are the very high quantum efficiency, 80% even at 800 nm, and the negligible thermal noise. The distance between the screen and the camera is about 1 meter. All components of the optical system can be inserted and remotely moved out from the optical axis using a remote control.

3. Emittance measurements

The measurements were performed at the FLASH free-electron laser user facility [14] at DESY (Hamburg). FLASH consists of an electron source to produce a high quality electron beam, followed by a superconducting linac with TESLA-type accelerating modules, and an undulator section to produce FEL radiation. Our experimental station was located in a beam line thus bypassing the undulators. During our measurements the electron beam energy was 1 GeV. The
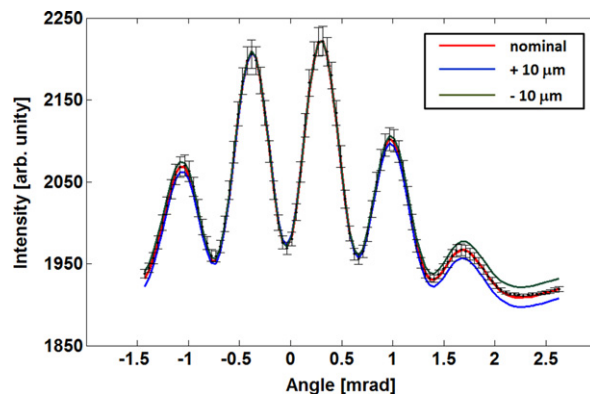
Figure 3. Measured ODRI angular distribution (black points) with a superimposed fit (red line). A value of beam size larger than 10 μm is shown in blue, while a beam smaller than 10 μm is shown in green. The cut on the left is due to a stray light background.

electron bunch train repetition rate was 10 Hz with typically 20 bunches per train. In our experiment, we used an electron bunch charge of 0.2 nC, and a CCD integration time of 2 seconds resulting in a total integrated charge of 80 nC. The complementary OTR measurements were carried out with a single 0.2 nC bunch to avoid damages on the conventional aluminum coated OTR screen.

3.1. Data analysis

The data analysis consists of multiple steps. The effects of the electron beam parameters were taken into account through the convolution of the ODRI angular distribution, as produced by a single particle, with two Gaussian distributions, one for the beam size and the other one for the angular spread. The whole beam was simulated by adding 5000 randomly generated distributions produced by single particles each one with different vertical position and incident angle. The chosen random distribution was a normal one, since it corresponds to the most likely one for an electron beam properly matched and tuned in a high energy linac. This assumption has been verified experimentally for the transverse profile. A Monte Carlo approach was then used to numerically solve the resulting expression which cannot be solved analytically. The obtained results were entered into the *Minuit* [15] routine. New distributions were generated through the Monte Carlo code; each time the fitting procedure changes the starting parameters. We fit seven parameters: the beam size and divergence, a constant background, the distribution center, the relative position of the beam inside the first and the second slit and the focal length of the optical system.

As we already mentioned, our model uses the far field approximation for the angular distribution. This approximation is valid when the slit's displacement is very small (about 25 μm), as was the case in our experiment. To test the validity of our analysis we measured several ODRI angular distributions with different observation wavelengths and radiation polarizations [16].

Figure 3 shows an example of a measured profile of the ODRI angular distribution superimposed with a fit, showing an excellent agreement between the model and the measurement data. This data is recorded during the quadrupole scan reported below and it refers
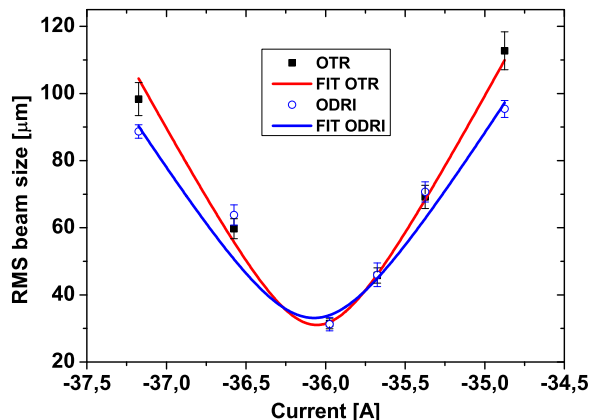
Figure 4. Comparison between quadrupole scans obtained by imaging a single electron bunch using the OTR screen and using the ODRI angular distribution produced by a long train of bunches going through the slits.

to the current value of −35.7 A in figure 4. In addition, simulations of the angular distributions, having different sizes of ±10 μm with respect to the nominal value, are shown in figure 3.

We use as an error estimate the Poisson noise of emitted ODRI photons after background subtraction, assuming that the CCD was operated in the photon counting regime as it was the case in our experiment. The cut in the left hand side of the profile is caused by the stray light background.

3.2. Measurement results

The transverse emittance was measured by means of the quadrupole scan technique [1], using the last quadrupole upstream of the experimental set-up. In order to validate the ODRI results, the quadrupole scan was also performed using conventional OTR imaging.

The two quadrupole scans are compared in figure 4. In the appendix, we show for each data point of figure 4 the 2D ODRI data images and the fit results as well as the beam spots obtained by OTR imaging.

For each value of the quadrupole current, we collected two ODRI angular distribution patterns. The two measurements differ only in the position of the first slit, which was moved by 25 μm with respect to the second one. In this way we obtained two data sets with only one parameter changed, i.e. the offset of the electron beam with respect to the center of the first slit. This constraint on the fit improves the confidence in the results. All ODRI distributions presented in this publication have been collected using the vertical polarizer and an interferential filter at 500 nm.

The standard deviation of the rms (root mean square) beam size has been used as the measurement error for the OTR data. In the ODRI case the error analysis is more complicated. Due to the stochastic nature of the fitting routine, *Minuit* is unable to perform a correct error analysis. Therefore, in order to have an error estimation for the ODRI measurements, we calculated the normalized χ^2 value of the fit and we varied the beam size parameter until the χ^2 changed by one unit. The change of the beam size causing one unit change of χ^2 is then used as an estimate for the beam size error in the ODRI measurements [17].

The resulting emittance is $\epsilon = (2.3 \pm 0.4)$ mm mrad for the ODRI measurements and $\epsilon = (2.4 \pm 0.4)$ mm mrad for the OTR measurements. The agreement between the two techniques is excellent, concerning both the measured emittance as well as the shape of the quadrupole scan curve (figure 4). The measurement error above, both for the ODRI and OTR measurements, is the RMS statistical error due to a shot-to-shot instability of the electron beam size and position. Since our experiment is located downstream of a complicated dogleg-like bend, we believe that this instability is mainly caused by only partially closed dispersion.

The resolution, independent of the measurement method, is an important issue when measuring small emittances with beam sizes down to 10 μm. The achievable ODRI resolution depends on several parameters such as the electron beam energy, the observation wavelength and the slit dimension. As a rule of thumb, the stronger the diffraction effect, i.e. the more the ODRI angular distribution differs from the OTR angular distribution, the better the resolution. The authors of [10] showed that for their experimental conditions (energy = 1.28 GeV, slit aperture = 260 μm, wavelength = 530 nm), they were able to measure a 10 μm beam size. They found a good agreement with independent measurements from a wire scanner at the same experimental location. Since a larger slit aperture improves the resolution, while a longer wavelength degrades it, we can assume that the resolution of our ODRI setup is of the same order of magnitude as measurements reported in [10].

4. Wakefield's calculation

In order to verify that the ODRI based diagnostics is not only non-intercepting but also non-disturbing, we have calculated the transverse and longitudinal wakefields using CST Particle Studio [18] and their effects on the electron bunch under our experimental conditions by analytical methods.

The 3D electromagnetic code solves the Maxwell's equations in a given structure taking a Gaussian beam as the source of the fields. This means that we cannot determine the wakefield generated by a point charge, called as the Green's function of the structure, but only the wake potential of the entire bunch instead. However, in our situation this is not a limitation because we can still determine the effects of the induced electromagnetic fields on the beam dynamics by directly using the wake potential, since we can assume that the longitudinal bunch distribution does not change when passing through the slit structure.

Due to the asymmetry of our set-up, we cannot obtain the transverse wake potential per unit of displacement (dipole wakefield with an off-axis source and an on-axis test charge [19]), but instead we have simulated an on-axis bunch and evaluated the transverse electromagnetic fields on the bunch itself.

We have verified that the longitudinal wake potential is independent on the displacement between the two slits. An energy loss and an induced energy spread are the effects of the longitudinal wake potential on the bunch.

A Gaussian bunch shape with rms length of 7 ps and a charge of 200 pC at an energy of 1 GeV was used. The total energy loss and the energy spread have been evaluated with the use of the longitudinal wake potential given by CST and the Gaussian distribution. The results give an energy loss of 2.7 keV with an additional energy spread of 1.6 keV, which corresponds to a relative energy spread of $1.6 \, 10^{-6}$, at 1 GeV. This is negligible compared to the usual uncorrelated energy spread of the 1 GeV beam (in the order of 100 keV).

The expected effect of the transverse wake potential is to deflect the electrons inside the bunch. The evaluation of the deflection angle has been performed in [20] and [21] starting from the spectral angular distribution of an ultrarelativistic electron passing through a circular disk. As our geometry is more complicated with respect to the one investigated in the aforementioned references, with two slits tilted 45 degrees relative to one another, and also taking into account the interference at the two interfaces, we have resorted to the transverse wake potential given by CST, since both the papers state that their approaches agree with results obtained from the geometric wakefield model.

The average deflection, corresponding to an average kick received by the bunch when it crosses the slit system, results in a divergence of $3.6 \, 10^{-7}$ rad for the horizontal case, and $1.3 \, 10^{-7}$ rad for the vertical one. The latter is evaluated for a $50 \, \mu$m slit displacement. The divergence spread due to the dependence of the transverse wake on the longitudinal position along the bunch is $1.4 \, 10^{-7}$ rad for the horizontal plane, and $5 \, 10^{-8}$ rad for the vertical one (50 μm misalignment).

From the performed wakefield study we can conclude that, for all cases in our experimental scenario, the longitudinal and transverse wake potentials cause only a negligible contribution to energy spread and beam divergence. We would like, however, to point out that this is not a general result, but applies only to our experimental situation. For each new experiment, the wakefield effects should be evaluated taking into account the characteristics of the experiment. If required, the slit geometry may be modified such that the wakefield effects can be neglected. In addition, in order to keep the non-intercepting feature of the device and to ensure a large enough ODRI signal, the geometry (slit apertures and relative distance) must be customized for each experiment according to the expected electron beam parameters.

5. Conclusions

The angular distribution of the optical diffraction radiation interference has been used for the first time to measure the transverse emittance in a non-intercepting way. The ODRI measurements were compared with measurements performed using standard intercepting OTR imaging. The agreement between the results obtained with these two techniques was excellent. In addition, an estimation of the wakefields has been included in our analysis showing that, in our experimental scenario, their effect on beam parameters can be neglected. In this case, ODRI diagnostics is not only non-intercepting but also non-disturbing.
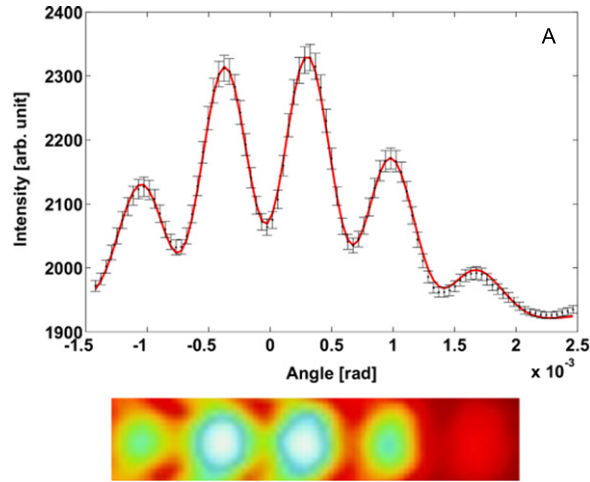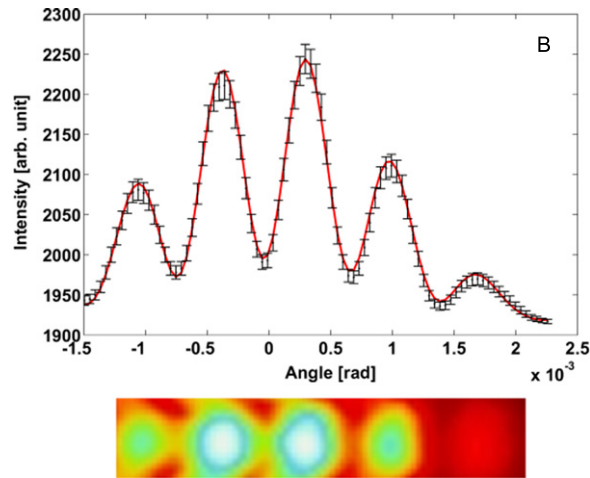
Acknowledgements

Figure A1. Top: angular distribution of the ODRI radiation at 500 nm with superimposed fit of data points; quadrupole current = −34.9A. Fit results: σ_y = 95.4 μm. Bottom: 2D angular distribution raw data.

Figure A2. Top: angular distribution of the ODRI radiation at 500 nm with superimposed fit of data points, quadrupole current = −35.4A. Fit results: σ_y = 70.7 μm. Bottom: 2D angular distribution raw data.

Appendix

We present here the experimental data for each point of the quadrupole scan in figure 4. Figures A1–A6 show the line profile of ODRI angular distribution along the central line. Figure A7 shows the beam spots obtained by single shot OTR imaging (please notice that due to a rotation of the camera the vertical dimension here is the horizontal one). The used quadrupole current and the measured rms beam size for each data point are given in the figure captions. The 2D raw data images are given for comparison as well.
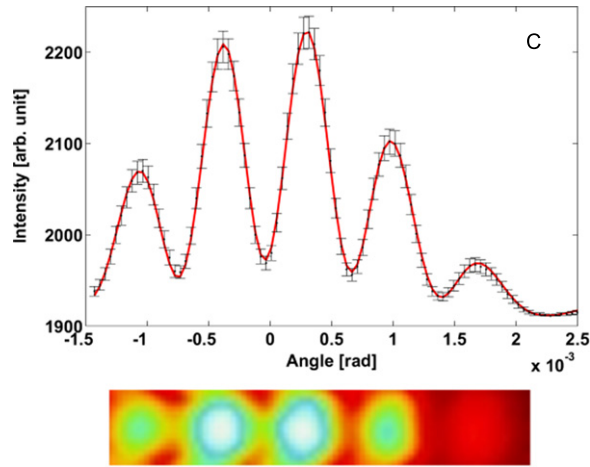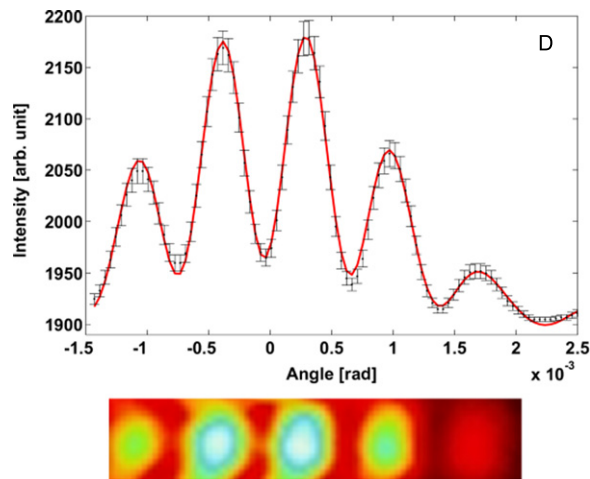
Figure A3. Top: angular distribution of the ODRI radiation at 500 nm with superimposed fit of data points, quadrupole current = −35.7A. Fit results: $\sigma_y = 46.0$ μm. Bottom: 2D angular distribution raw data.
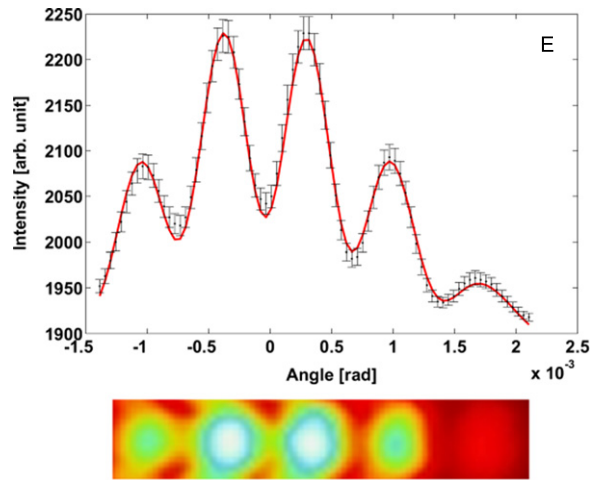

Figure A4. Top: angular distribution of the ODRI radiation at 500 nm with superimposed fit of data points, quadrupole current = −36.0A. Fit results: $\sigma_y = 31.3$ μm. Bottom: 2D angular distribution raw data.

Figure A5. Top: angular distribution of the ODRI radiation at 500 nm with superimposed fit of data points, quadrupole current = −36.6A. Fit results: σ_y = 63.8 μm. Bottom: 2D angular distribution raw data.
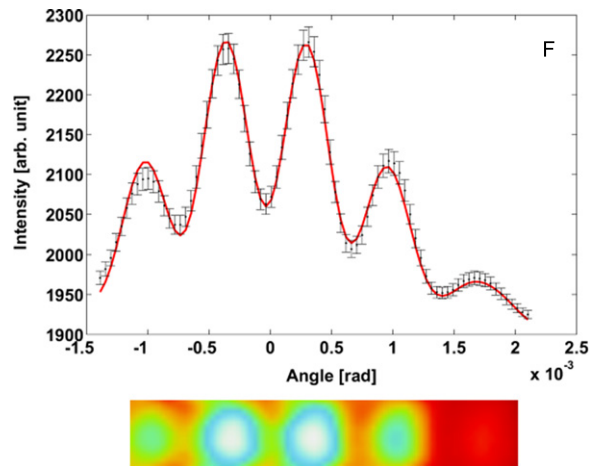

Figure A6. Top: angular distribution of the ODRI radiation at 500 nm with superimposed fit of data points, quadrupole current = −37.2A. Fit results: σ_y = 88.7 μm. Bottom: 2D angular distribution raw data.
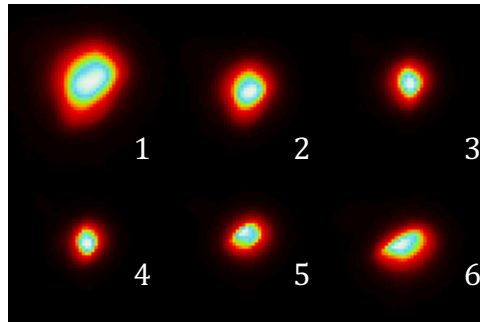
Figure A7. 1: Quad current $= -34.9$A, $\sigma_y = 112.7$ μm. 2: Quad current $= -35.4$A, $\sigma_y = 69.2$ μm. 3: Quad current $= -35.7$A, $\sigma_y = 45.8$ μm. 4: Quad current $= -36.0$A, $\sigma_y = 31.5$ μm. 5: Quad current $= -36.6$A, $\sigma_y = 59.7$ μm. 6: Quad current $= -37.2$A, $\sigma_y = 88.7$ μm.

References

[1] Minty M G and Zimmermann F 2003 *Measurement and Control of Charged Particle Beams* (Berlin: Springer)

[2] Ross M 2003 *Proc. Particle Accelerator Conf. (Piscataway, NJ: IEEE)* **1** pp 503–7

[3] Tenenbaum P and Shintake T 1999 *Annu. Rev. Nucl. Part. Sci.* **49** 125

[4] Castellano M 1997 *Nucl. Instrum. Methods Phys. Res.* A **394** 275

[5] Rule D, Fiorito R and Kimura W 1997 *AIP Conf. Proc.* **390** 510

[6] Ter-Mikaelian M L 1972 *High-energy Electromagnetic Processes in Condensed Media* (New York: Wiley)

[7] Potylitsyn A 1998 *Nucl. Instrum. Methods Phys. Res.* **145** 169

[8] Potylitsina-Kube N and Artru X 2003 *Nucl. Instrum. Methods Phys. Res.* **201** 172

[9] Potylitsyn A P, Ryazanov M I, Strikhanov M N and Tishchenko A A 2010 *Diffraction Radiation from Relativistic Particles* vol 239 (Berlin: Springer)

[10] Karataev P, Araki S, Hamatsu R, Hayano H, Muto T, Naumenko G, Potylitsyn A, Terunuma N and Urakawa J 2004 *Phys. Rev. Lett.* **93** 244802

[11] Cianchi A, Castellano M, Catani L, Chiadroni E, Honkavaara K and Kube G 2011 *Phys. Rev. ST Accel. Beams* **14** 102803

[12] Shpakov V and Dabagov S B 2012 *Tech. Rep.* INFN-12-02/LNF (arXiv:1408.5758)

[13] Cianci E, Notargiacomo A, Cianchi A and Foglietti V 2001 *Proc. SPIE* **4557** 242–9

[14] Vogt M, Faatz B, Feldhaus J, Honkavaara K, Schreiber S and Treusch R 2014 Status of the free electron laser user facility FLASH *Proc. 5th Int. Particle Accelerator Conf. (Dresden, Germany, 2014)* p 938

[15] James F 1994 *CERN Program Library Long Writeup* D506 (http://hep.fi.infn.it/minuit.pdf)

[16] Cianchi A, Balandin V, Castellano M, Catani L, Chiadroni E, Gatti G, Golubeva N, Honkavaara K and Kube G 2012 *J. Phys.: Conf. Ser.* **357** 012019

[17] Hughes I and HASE T 2010 *Measurements and their Uncertainties* (Oxford: Oxford University Press) pp 74–9

[18] CST AG, Darmstadt, Germany, http://cst.com

[19] Palumbo L, Vaccaro V G and Zobov M 1995 *Proc. CERN Accelerator School: Advanced Accelerator Physics Course* No. 95-06 ed S Turner (Geneva, Switzerland)

[20] Potylitsyn A *et al* 2005 *Nucl. Instrum. Methods Phys. Res.* B **227** 170

[21] Xiang D and Huang W 2007 *Phys. Rev. ST Accel. Beams* **10** 12801